IEICE TRANS. INF. & SYST., VOL.E99–D, NO.11 NOVEMBER 2016

LETTER

An Algorithm of Connecting Broken Objects Based on the Skeletons

Chao XU[†], ***Student Member***, **Dongxiang ZHOU**[†a)], ***and*** **Yunhui LIU**[††], ***Nonmembers***

SUMMARY The segmentation of Mycobacterium tuberculosis images forms the basis for the computer-aided diagnosis of tuberculosis. The segmented objects are often broken due to the low-contrast objects and the limits of segmentation method. This will result in decreasing the accuracy of segmentation and recognition. A simple and effective post-processing method is proposed to connect the broken objects. The broken objects in the segmented binary images are connected based on the information obtained from their skeletons. Experimental results demonstrate the effectiveness of our proposed method.

key words: *segmentation, tuberculosis, computer-aided diagnosis, post processing*

1. Introduction

Despite that the incidence of tuberculosis (TB) has decreased by an average of 1.5% per year since 2000, TB remains one of the biggest threats to the human survival. In 2014, 1.5 million people were killed by TB worldwide, and 6 million new cases were reported to WHO (World Health Organization) [1]. There are many new cases that were undiagnosed or were not reported to WHO. Early discovery and treatment are necessary for the control and treatment of TB. With the development of computer-aided diagnosis, TB can be diagnosed efficiently and accurately [2], [3]. The patients were diagnosed by analyzing the captured images of the sputum smear slides with the microscope, which can reduce the massive screening work and improve the accuracy of diagnosis.

The segmentation of Mycobacterium tuberculosis (MTB) images aims to extract the suspicious MTB objects, which is prepared for the recognition and counting in the next step. A framework of MTB recognition based on active shape model (ASM) was proposed [4]. In this framework, a segmentation algorithm using the marker-based watershed transform was utilized to extract the candidate objects. Good segmentation results can be obtained by the segmentation algorithm in the images with different background colors. However, sometimes the segmentation results of MTB objects are broken. One of the reasons is that the contrast of some MTB objects is too low, which is caused by the low quality of the captured images. Another reason is the limits of segmentation method. MTB belongs to the rod-shaped object with various bending deformation. The shapes of the broken MTB objects are similar to the integrated MTB objects. Therefore, the emerging broken MTB objects would increase the false positive rate of the computer-aided diagnosis system.

This paper proposed a method of connecting the broken MTB objects in the segmented images. The shape characteristics of the MTB objects can be represented by their skeletons. The endpoints and other relative information, extracted based on the skeletons of the objects, were used to connect the broken objects. The detailed process is presented in Sect. 2.

2. Methods

2.1 Skeleton and Endpoints Information Extraction

The skeleton of an object is a line with one-pixel width in the binary image. The shape and topological structure of the line are the same with those of the object. Therefore, the skeleton is a simplified description form for the shape of the object. The MTB is a non-rigid, rod-shape object. The bending ways and degrees of the objects' shape can be represented by the skeletons.

The skeleton is generated with the morphological thinning method [5]. The thinning process can be defined by the hit or miss transform, which is given by [6]

$$A \otimes B^i = A - (A \circledast B^i) \tag{1}$$

where $\otimes$ denotes the thinning operation; $\circledast$ denotes the hit or miss transform; B^i is the structure element sequence, $i \in [1, n]$ and n is the number of structure elements. The thinning process of the set A is performed by the whole structure elements from the sequence until A is not changed after traversing the structure elements. Figure 1 is an example of the obtained skeletons. The first and second row show the single and touching MTB objects respectively. The points at the end of the skeletons are named endpoints in this paper. For each single MTB object, there are two endpoints on the skeleton. The endpoints have a certain distance to the edge of the object. In Fig. 1 we can see that the basic shape and bending deformations can be adequately represented by the skeletons.

Given the skeleton, the vertices and edge points at the

Manuscript received June 2, 2016.
Manuscript revised July 27, 2016.
Manuscript publicized August 10, 2016.

[†]The authors are with the College of Electronic Science and Engineering, National University of Defense Technology, Changsha 410073, China.
[††]The author is with the Department of Mechanical and Automation Engineering, The Chinese University of Hong Kong, Hong Kong, China.
a) E-mail: dxzhou@nudt.edu.cn (Corresponding author)

DOI: 10.1587/transinf.2016EDL8117

Copyright © 2016 The Institute of Electronics, Information and Communication Engineers

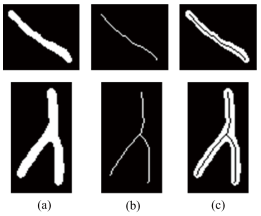


Fig. 1 The skeletons of the MTB objects. (a) is the binary images. (b) is the obtained skeletons. (c) shows the skeletons and objects together (the black lines in the white areas are the skeletons).

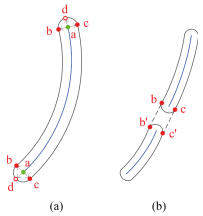


Fig. 2 The definition of vertices and edge points. (a) shows the vertices and edge points of the skeleton. The blue line is the skeleton, and the green points a are the endpoints on the skeleton. The red solid points b and c are the edge points, and the red hollow points d are the vertices of the object. (b) is the sketch map of connecting two broken objects. The edge points are used to connect the two objects.

ends of the object can be defined, as shown in Fig. 2. In Fig. 2, the edge points b and c can be considered as the transition points between the ends and the middle part of the object. The distance between b and c is close to the object width. Vertex d is the point with large curvature at the ends of the object. Figure 2 (b) shows the principle of our proposed method. The closed region is obtained by connecting the corresponding edge points from two different objects. Then the integrated object is generated from the process of region filling. The way of finding the vertices and edge points is detailed as follows.

- The endpoint of the skeleton is first located based on the skeleton. The slope of the endpoint is computed according to its k nearest neighborhood point on the skeleton. The tangential and normal directions are quantized to 16 neighborhood.
- The vertices are the specific intersection points, which are obtained by extending the endpoint to the object boundary along the tangential directions.
- The edge points are the specific intersection points, which are obtained by extending the endpoint to the object boundary along the normal directions.

k is set 3 to avoid the impact of non-smooth skeletons. Given the binary images obtained by the segmentation, the skeleton analysis is performed with all the objects. The endpoints, tangential directions, edge points, and vertices are extracted based on the described method. The average gray values of the skeleton pixels are also computed in this step. The gray channel is given by

$$gray = R * 0.299 + G * 0.587 + B * 0.114 \quad (2)$$

where R, G, and B denote the red, green, and blue channels respectively.

2.2 Broken Objects Searching

The broken objects produced by the segmentation belong to the same objects in the input images. Therefore, only the two regions from the same object need to be connected. The distance between the endpoints are close, and the angles between the skeletons are small. The critical step of the proposed method is searching the broken objects from the binary image. The detailed process is as follows.

(a) Extend p pixels from the vertex d of one region (denoted as A) along the tangential direction until intersects another region (denoted as B) at point s. If the intersection s is not existent, continues this step with other vertices, otherwise go to (b);

(b) Compute the mean gray values of the pixels from line ds, denoted as M_{ds}, and compare the average gray values of the skeleton pixels, denoted as M. If $|M_{ds} - M| < T$, then go to (c), otherwise go to (a);

(c) Judge the two regions whether they have been connected by querying the connection records. If they have been connected, then go to (a), otherwise, find out the nearest vertex d' to the intersection s from the region B, and go to (d);

(d) Compute the distances from the vertex d' to the corresponding edge point c' and the intersection s respectively, denoted as $d'c'$ and $d's$. If $d'c' < r \cdot d's$, $r \in [0, 1]$, it indicates that the intersection s is not nearby the vertex d', go to (a), otherwise prepare to connect these two regions using the obtained edge points.

In step (a), the extending distance $p = 10$ can satisfy the requirement of connecting broken objects. The purpose of step (b) is to avoid connecting the two objects which have the short distance but do not belong to the same object. The difference between the average gray value of the skeleton and the extending trajectory is introduced to judge whether the two objects are the broken objects or not. The background pixels are filled between the non-broken objects, and their average gray value has a large difference in the pixels of the objects. The difference threshold T is set to 19. The connection records are used in step (c) to avoid repeating connection. Therefore, in the process of connecting, the information about the endpoints (including the number, tangential directions, etc.) in the skeletons requires no updates after they are connected. The connection status between the skeletons is saved in the connection records. This will not be influenced by the processing order of the skeletons. In this case, we only need to traverse the whole regions in the binary image for one time. The efficiency of the proposed method can be improved. In step (d), the distances from the vertex to the edge point and the intersection point are compared to judge whether the connection position occurred at the ends of the objects. Considering the errors caused by the smoothness of object boundaries and the computation of tangential directions, the parameter r is set to 0.7.

2.3 Broken Objects Connection

Given the two objects which need to be connected, the way of connection between the edge points are first determined by comparing their angles, as shown in Fig. 2 (b). The smaller angle between the two lines is considered as the right way of connection. It ensures that the generated contours are reasonable and closed. After that, the region filling is utilized to obtain the integrated objects. Finally, the connection records from the two connected areas is updated to improve the efficiency of broken objects searching and to avoid repeating the operation.

3. Experimental Results and Discussion

The proposed method was performed by Matlab 2015a. The test images were captured from the sputum smear slides using the light microscope. Some experimental results are shown in Fig. 3.

In Fig. 3, the color of the pixels of some objects is not uniform. The color of the middle part of the objects is too light, which results in broken objects by the segmentation. The broken objects are marked by the black rectangles in Fig. 3 (a). The corresponding objects are broken in Fig. 3 (b). This problem can be solved by our proposed method. From Fig. 3 (c) we can see that the ends of the broken objects are connected to the integrated objects. The width of the newly added regions is almost the same as that of the objects. Therefore, the shape of the connected objects is preserved well. Moreover, only the extension of one skeleton intersects with another one near the endpoint is considered. The purpose is to ensure the connection rationality, as shown by the blue rectangle. The two objects marked by the green rectangle are non-broken objects. Although their endpoints have the short distance, and the intersection point near the endpoint of the other skeleton, they were not connected by the proposed method. Thus, the over-connection is effectively avoided.

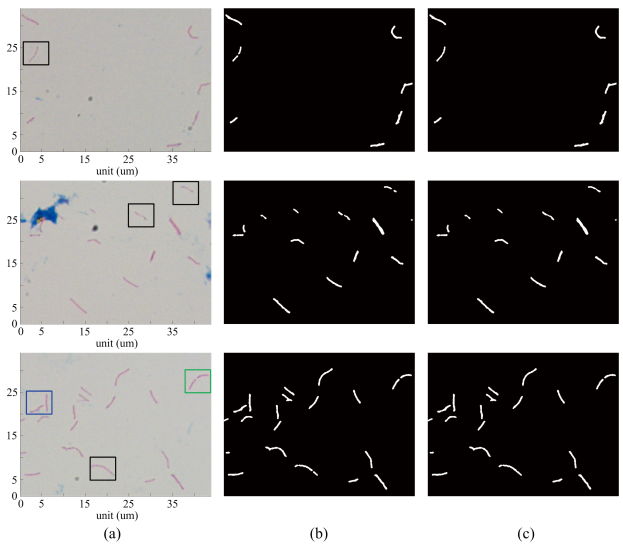


Fig. 3 Results of the broken objects connection. (a) is the input images. (b) is the segmentation results with broken objects. (c) is the results of broken objects connection

3.1 Quantitative Evaluation

We tested 12 images that contain the broken objects. Each image has a resolution of 680×512 pixels. The segmentation algorithm introduced in [4] was used. For these images, a total of 17 broken objects appeared in the segmentation results, and 14 of them were fixed by our proposed algorithm. The success rate is 82.35%. The characteristics of the fixed objects satisfy the requirements as mentioned in Sect. 2.2. The remaining three broken objects were not fixed. One of them was caused by the overlong distance between the endpoints. The other two were affected by the smoothness of the ends, resulting in the miss of the intersection points. The over-connection did not occur during the process of connecting. The experimental results indicate that most of the broken objects can be fixed by the proposed algorithm.

The sensitivity, specificity, and accuracy are applied for evaluation from another aspect, which are given by

$$\begin{aligned} SEN &= \frac{TP}{TP+FN} \times 100\% \\ SPE &= \frac{TN}{TN+FP} \times 100\% \\ ACC &= \frac{TP+TN}{TP+TN+FP+FN} \times 100\% \end{aligned} \tag{3}$$

where SEN, SPE, and ACC denote the sensitivity, specificity, and accuracy respectively. TP, FP, TN, and FN denote the number of true positive, false positive, true negative, and false negative objects respectively. The statistical variables such as TP and FP are obtained by comparing the detected results with the ground truth, which was given by expert pathologists. For example, adding 1 to TP when the marked positive object is judged as the MTB object.

The recognition results of the 12 images are obtained by the algorithm [4], as shown in Table 1. The first row is the original result without the step of broken objects connection [4], and the second row is the result processed by our proposed algorithm. The proposed algorithm achieves a better result than the algorithm [4], especially in terms of the specificity. The broken objects connection can reduce the number of FP in recognition. Therefore, the specificity can be largely improved. The specificity values are not very high, because there is a bit of debris (TN) in the tested images. Although the sensitivity values are almost equal, the proposed algorithm gives higher accuracy value than the algorithm [4]. The algorithm [4] can obtain good results. Our

Table 1 Results of quantitative evaluation.

Method	SEN (%)	SPE (%)	ACC (%)
Orig.	93.33	18.18	88.20
Prop.	93.37	28.57	90.51

proposed algorithm is an improvement to the algorithm [4]. Therefore, the improvement of accuracy can indicate the effectiveness of our proposed algorithm. The proposed algorithm can improve the accuracy of object recognition by reducing the impact of image quality and segmentation algorithm. Therefore, the reliability of the computer-aided diagnosis of TB can be improved.

4. Conclusion

The broken objects are presented in the process of segmentation due to the low-contrast objects and the limits of segmentation method, which would decrease the accuracy of segmentation and recognition. This paper proposed a method of broken objects connection based on the skeletons to solve the problem. The ends of the broken objects are connected by the proposed method, and the shape of the connected objects are consistent with that of the MTB objects. Meanwhile, the over-connection problem can be avoided. Experimental results demonstrate the effectiveness of the proposed method.

References

[1] World Health Organization, "Global tuberculosis report 2015," Global Tuberculosis Report, 2016.
[2] K. Veropoulos, C. Campbell, and G. Learmonth, "Image processing and neural computing used in the diagnosis of tuberculosis," Proc. IEE Colloquium on Intelligent Methods in Healthcare and Medical Applications (Digest no.1998/514), York, UK, pp.8/1–8/4, 1998.
[3] J. Chang, P. Arbeláez, N. Switz, C. Reber, A. Tapley, J.L. Davis, A. Cattamanchi, D. Fletcher, and J. Malik, "Automated tuberculosis diagnosis using fluorescence images from a mobile microscope," Medical Image Computing and Computer-Assisted Intervention, MICCAI 2012, Lecture Notes in Computer Science, vol.7512, pp.345–352, Springer Berlin Heidelberg, Berlin, Heidelberg, 2012.
[4] C. Xu, D. Zhou, T. Guan, Y. Zhai, and Y. Liu, "Automatic recognition of mycobacterium tuberculosis based on active shape model," IEICE Trans. Inf. & Syst., vol.E99-D, no.4, pp.1162–1171, April 2016.
[5] R.C. Gonzalez and R.E. Woods, Digital Image Processing, 2nd ed., Prentice Hall, New York, 2002.
[6] P. Soille, Morphological Image Analysis: Principles and Applications, 2nd ed., Springer-Verlag, 2008.